Biomechanical Responses of Small Female PMHS Subjected to Abdominal Loading

Rakshit Ramachandra, Yun-Seok Kang, Jason Stammen, Ellen Lee, Kevin Moorhouse, John Bolte IV

Abstract Several studies have provided a valuable assessment of the abdominal responses of mid-sized adult males. The objectives of this study were to evaluate the biomechanical responses of small female occupants when subjected to abdominal loading using post-mortem human subjects (PMHSs) and develop biofidelity targets. A total of nine unembalmed PMHSs, with an average mass and stature of 51±8 kg and 163±9 cm, respectively, were subjected to one of two mid-abdominal loading scenarios: fixed-back belt pull at 4 m/s and rigid bar impact at 6 m/s. The abdominal vasculature was pressurised, and pressure transducers were used in both abdominal aorta and inferior vena cava (IVC). In two of the nine tests, ruptured kidneys and tears in the jejunum, duodenum and splenic capsule were present. The other seven tests resulted in no organ injury. Abdomen biofidelity response targets for fixed-back belt pull and free-back rigid bar loading were created for evaluating and improving the biofidelity of small female-sized surrogates. Various biomechanical variables were calculated and compared to a previously obtained blunt impact and belt loading dataset.

Keywords Abdomen, female, belt, rigid bar.

I. INTRODUCTION

Abdominal injuries are amongst the most common types of Abbreviated Injury Scale (AIS) 4+ injuries in frontal, farside, and nearside crashes according to a study of the National Automotive Sampling System – Crashworthiness Data System (NASS-CDS) [1]. The abdomen, along with the head and thorax, represent the three most frequently and severely injured body regions in motor vehicle crashes (MVC). The most frequently injured organs for drivers in frontal crashes were the spleen and liver, and for front passengers were the jejunum-ileum, spleen, and liver, based on crash data from the United Kingdom Co-operative Crash Injury Study (CCIS) [2].

Impact and injury response of the abdomen has been studied under various loading conditions, often using post-mortem human subjects (PMHSs). Several studies with PMHSs or animal models have correlated measured response parameters with injury outcomes [3-15]. Although these previous studies included data from both male and female specimens, the subjects were predominantly male since the focus for those studies was on understanding mid-size male injury response and tolerance.

While previous studies provide a valuable assessment of injury tolerance of the mid-sized adult male, real world MVCs include occupants of different sex, age and size. Some studies have suggested that females may generally be at greater risk of AIS 2+ and 3+ injuries compared to males in similar crash scenarios [16-18]. However, in terms of abdominal injuries, it is unclear if the higher risk to female occupants is related to a lower injury tolerance, a mechanism of injury due to their preferred seated posture (closer to the wheel), or an increased submarining risk due to smaller stature. These are important factors to determine whether the abdomen response targets used for anthropomorphic test devices (ATDs) or human body models (HBMs) [19-20] representing male and female occupants should be different.

Due to limited sex- and size-specific data, surrogates such as the Test Device for Human Occupant Restraint Fifth Female (THOR-05F) ATD and small female HBMs are often evaluated against response data from mid-sized male testing that have been scaled using simplified scaling techniques [21-22] not explicitly developed for use towards abdomen response. Collecting sex- and size-specific abdominal response data will benefit the development of a biofidelic abdomen in these ATDs and HBMs. The objective of this study was to determine the responses of small female-sized PMHSs when subjected to abdominal loading and develop biomechanical targets

R. Ramachandra is a Research Scientist at Transportation Research Center Inc, East Liberty, OH, USA (+1 313 460 9914 and r.ramachandra.ctr@dot.gov). YS. Kang and JH. Bolte IV are Faculty at the Injury Biomechanics Research Center at The Ohio State University, Columbus, OH. USA. J. Stammen and E. Lee are Engineers and Contracting Officers, K. Moorhouse is Division Chief of Applied Biomechanics at National Highway Traffic Safety Administration, U.S. Department of Transportation, Washington, DC, USA.

to benchmark ATDs and HBMs.

II. METHODS

A total of nine PMHSs were tested in one of two loading conditions. Fixed-back belt loading tests (6 PMHSs) and rigid bar impacts (3 PMHSs) were conducted to generate abdominal responses relevant to a small female occupant. The loading conditions were selected with the future intent of constructing abdominal injury risk functions from injurious and non-injurious loading tests, while also allowing for development of biomechanical response corridors as outlined in the current study.

PMHS Selection and Preparation

A total of nine PMHSs were obtained through the Ohio State University's Body Donor Program with their use approved by the Body Donor Program's Advisory Committee. All specimens were screened for infectious diseases, and a dual energy X-ray absorptiometry (DXA) scan was used to exclude specimens with osteoporosis (T-score acceptance criteria > -2.5). Specimens were required to have a body mass index (BMI) of less than 24.9 kg/m^2. Specimens that had major abdominal scars or a history of abdominal disease were also excluded. A computed tomography (CT) scan was done prior to acceptance of each PMHS to check for pre-existing issues such as fractures or artificial implants.

Testing on eight of the nine PMHSs was performed within 72 to 120 hours post death (only SB01 was frozen fresh). The specimens were stored in a cooler overnight and brought to room temperature of 21C prior to testing. Anthropometry of each PMHS was recorded, including abdominal depth, circumference, and width. Prior to installing instrumentation, warm saline was flushed through both arterial and venous systems to clear blood clots from the abdominal aorta and IVC. However, the bladder and colon were not evacuated.

Table I shows the pre-test characteristics of each tested PMHS. Average mass and seated abdominal depths were very close to the THOR-05F dimensions. Test SB02 was conducted on a male specimen who fitted the anthropometric criteria of the test group, given the difficulty of procuring specific-sized specimens. All other specimens were female.

TABLE I
SPECIMEN INFORMATION

Test	Test Condition	Age/Sex	Mass (kg)	Stature (cm)	Abd C'ference (cm)	Seated Abd Depth (cm)	BMI (kg/m^2)
SB01	Fixed-Back Belt	38F	54	172.0	72.5	21.8	18.3
SB02	Fixed-Back Belt	73M	61	175.0	76.0	20.5	21.6
SB03	Fixed-Back Belt	86F	43	154.5	71.5	26.5	18.0
SB05	Fixed-Back Belt	83F	55	175.5	68.0	21.8	17.9
SB06	Fixed-Back Belt	95F	55	156.0	90.0	25.0	22.6
SB07	Fixed-Back Belt	102F	37	152.4	60.8	21.2	15.9
RB01	Rigid Bar	80F	61	165.1	81.0	24.3	22.3
RB02	Rigid Bar	77F	45	160.0	73.5	18.5	17.6
RB03	Rigid Bar	57F	51	159.0	78.5	23.3	20.2
Average		77	51	163.3	74.6	22.5	19.3
± 1 Std Dev		19.5	8.1	9.0	8.3	2.5	2.4
THOR-05F			*50*	*151.0*	*86.5*	*22.5*	*21.9*

Fixed-Back Belt Loading Test Setup

For the belt loading test setup, the PMHS were seated on a table with their back upright against support plates used to arrest spinal motion. The head was supported by a halter connected via a ratchet strap to the frame of the fixture. The seatbelt was wrapped around the anterior and lateral aspects of the PMHS abdomen at the mid-abdomen level. Anteriorly, this position corresponded to the umbilicus of the specimen. Both sides of the seatbelt, posterior to the specimen, were kept parallel to each other at a distance equal to the seated abdomen width of the PMHS. Initial belt tension was adjusted so that each seatbelt load cell measured 10-20 N, to ensure a repeatable initial position of the belt. The upper arms and elbows of the specimens were lifted to shoulder level to ensure they would not interfere with the movement of the PMHS. The spine was positioned to be upright with the back of the PMHS flush against the mounting plates to minimise spinal flexion/extension during impact. The

legs were splayed slightly outward in a natural seated position. The seatbelt loading device previously described in [11] was modified to accommodate the back-support plates to mimic the fixed-back belt loading to mid-sized male specimens [8]. The abdominal region of each specimen was loaded by the seatbelt at a nominal velocity of 4 m/s. Both arterial and venous systems in the abdomen were re-pressurised using saline before each test to approximate physiological levels (14.0 kPa in the aorta and 0.9 kPa in the IVC). Pre-test positioning in the belt pull test apparatus is shown in Figure 1, and schematics of the setup are provided in Figure A1.

A total of six tests, one test per PMHS, were conducted in this configuration. Three of the tests were intended to not induce abdominal injuries by limiting the compression of the abdomen to approximately 27% of the specimen's seated abdominal depth. This stroke restriction was based on non-injurious compressions reported in a previously conducted submarining test series [8] and is referred to as lower-compression (LC) in this paper. The other three tests were designed to produce abdominal injuries by allowing a longer pull of approximately 50% of the specimen's abdominal depth, and the corresponding stroke is referred to as higher-compression (HC).

Free-Back Rigid Bar Loading Test Setup

For the rigid bar test setup, the PMHS were seated in a free-back upright configuration with the impact aimed at the mid-abdomen at the level of the umbilicus. The impactor loading device was designed to mimic the [3] mid-abdominal impacts to mid-sized male specimens. A 2.5 cm diameter, 30 cm wide rigid bar impactor was attached to the ram shaft by means of a six-axis load cell to measure impact force. Total mass of the impactor was 23 kg, scaled down from 46 kg used in [3] to accommodate small female specimens. The impact speed of the bar was approximately 6 m/s.

Pre-test positioning of a specimen in the rigid bar impact test apparatus is shown in Figure 2. The PMHSs were seated on a Teflon skid in the same position as in the belt tests, again using a head halter connected to an electromagnet release system that was activated just prior to event. Strips of conductive tape were placed on both the specimen's abdomen and the impactor face. When contact between conductive tapes occurred, the data acquisition system was triggered and time zero defined. The rigid bar made initial contact with the PMHS approximately at the level of the umbilicus or third lumbar vertebra (L3). A total of three tests, one test per PMHS, were conducted in this configuration. These tests were designed to not induce injuries by restricting the ram stroke to a length of approximately 27% of the specimen's seated abdominal depth.

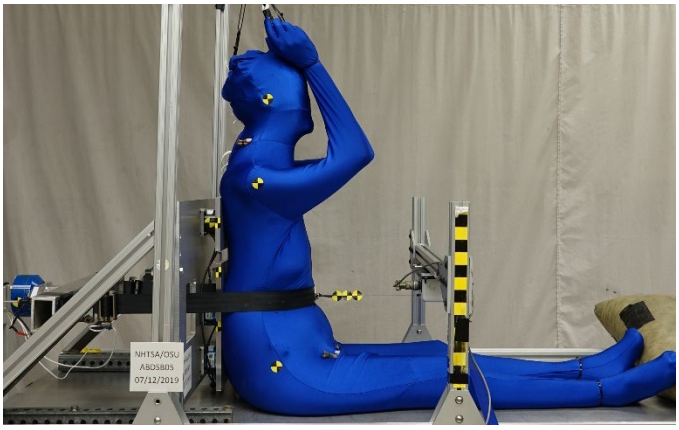

Fig. 1. Belt loading test setup.

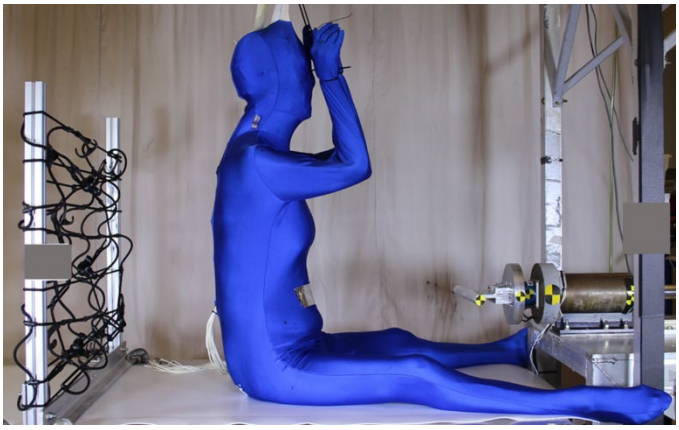

Fig. 2. Rigid bar impact test setup.

Instrumentation

Internal instrumentation included pressure transducers (Millar Instruments, TX, USA, Model #SP-524) attached to angiographic catheters routed through Foley catheters. The methodology followed the description in [11]. Pressure transducers were inserted into the inferior vena cava (IVC) and abdominal aorta. For spinal motion, six degree-of-freedom (6DX) motion blocks consisting of three accelerometers and three angular rate sensors (DTS, CA, 6DX PRO 2K-18K) were fixed to vertebrae T8, T12, L3, and L5 using bridge mounts that rested on the pedicles of the respective vertebrae with one screw drilled through the vertebral body. The L3 motion block aligned vertically with the impact location. Abdominal depth and width measurements were retaken after positioning the specimen to adjust the belt width and ram stroke.

Injury Assessment

Following each test, a post-test computed tomography (CT) scan was taken to document the change in locations of the internal instrumentation as well as any injuries that occurred. An anatomical dissection was then conducted to note all injuries in detail. Injury severity scores were assigned based on Abbreviated Injury Scale 2005 – update 2008 [23].

Data Analysis

Data were acquired at a sampling frequency of 20,000 Hz using TDAS G5 or SLICE PRO (DTS, CA, USA), and all signals were filtered according to standard SAE-J211. Data from the 6DX motion blocks were transformed to the laboratory coordinate system (LCS)according to SAE-J211. For the belt pull tests, time zero was defined as 0.5g acceleration of the pneumatic ram.

Force applied to the abdomen in the belt pull tests was calculated as the sum of two tension seatbelt load cell forces. In the rigid bar tests, the impact force was measured by the six-axis load cell installed between the ram shaft and the impactor face. Abdomen penetration was defined as the deflection of the abdomen versus time, where deflection is measured at the point anterior to the abdomen at the sagittal midline. To account for the variation of abdominal depth between PMHSs, abdomen compression was calculated by dividing abdominal penetration by seated abdominal depth at the time of testing (Table I). In the belt loading tests, abdomen penetration was measured by an anterior string potentiometer (Celesco, CA, USA, Model #PT101) (Eq. 1). For the rigid bar tests, abdomen penetration was calculated by subtracting the displacement of the lumbar spine at the level of the impact (L3) from the displacement of the ram measured via a linear potentiometer upon contact (Eq. 2).

$$\delta_{Abd} = \delta_{Belt} \quad (1)$$

$$\delta_{Abd} = \delta_{Ram} - \iint a_{X(L3)} \quad (2)$$

where, δ_{Abd} = abdomen penetration (mm); δ_{Belt} = displacement of seatbelt relative to table fixture (mm); δ_{Ram} = displacement of ram (mm); and $\iint a_{X(L3)}$= displacement of L3 calculated using x-accelerometer (mm). Abdomen penetration speed was found by differentiating abdomen penetration filtered using CFC60.

Abdomen arterial and venous pressures were recorded in all PMHS tests. Due to the lack of a standard filter class for pressure data, a fast Fourier Transform (FFT) analysis of the pressure signals was performed to determine that filtering at CFC60 was appropriate [11][15]. The peak rates of pressure change, $\dot{P}_{max}$, and the product of peak pressure and peak rate of pressure change, $P_{max}*\dot{P}_{max}$, were calculated from the venous pressure signals.

Abdominal biofidelity response targets were developed for the three loading conditions: fixed-back belt pull (LC), fixed-back belt pull (HC), and free-back rigid bar impact (LC). The force and compression responses were first moved into a common time interval basis using interpolation. These force and compression responses were then averaged across the three tests within each of the three loading conditions at every time interval to calculate the mean and standard deviation. The upper and lower boundaries for compression and force were calculated by adding the standard deviation to the mean value at each time for the upper bound and subtracting the standard deviation from the mean value at each time for the lower bound.

III. RESULTS

Fixed-Back Belt Loading Test

Force-time and penetration-time histories for the PMHS tested in the belt loading condition are shown in Figures B1 and B2. In tests SB01-03 that were intended to be non-injurious, peak seatbelt forces and penetrations ranged from 1.9 to 2.6 kN and 65 to 94 mm, respectively. Peak abdomen compression ranged from 23 to 28% with a mean compression of 25% among these tests. In tests SB05-07 that were intended to be injurious, peak seatbelt forces and penetrations ranged from 4.4 to 5.5 kN and 70 to 118 mm respectively. Peak compression of the abdomen ranged from 36 to 50% with a mean compression of 45% among these tests.

The peak pressure values recorded in the IVC transducers ranged from 17.5 to 99.2 kPa in the lower-compression tests and 39.7 to 245.0 kPa in the higher-compression tests. The IVC pressure transducer with the highest peak (positive maximum) pressure was defined as P_{max} for purposes of injury prediction. The positive maximum rate of pressure change ($\dot{P}_{max}$) in the IVC during the event up to the time of P_{max} ranged from 0.84 to

8.02 kPa/ms in lower-compression tests and 2.80 to 31.50 kPa/ms in higher-compression tests. The values of peak pressures from all transducers in the abdominal vasculature are included in Table BI.

Figures 3 and 4 show belt force vs. abdomen compression responses. Force vs. abdominal penetration responses are shown in Figure B5. The force and penetration responses were not normalised since the specimens were controlled to match the target demographic of a fifth percentile female. High-speed video demonstrated that, especially in the non-injurious intent tests, the seatbelt string pot continued to displace beyond peak force. This was due to inertial effects upon the sudden arrest of ram stroke, leading to additional spooling out of the string potentiometer. This over-spooling occurred after the loading event and beyond the period of interest, and hence the data were considered accurate until peak force was measured. Since abdominal depths varied between PMHSs at the time of testing, penetration values were normalised by seated PMHS abdominal depth shown in Table I.

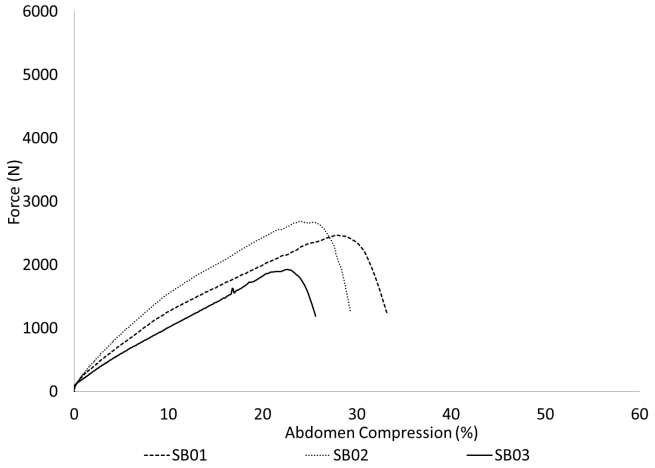

Fig. 3. Belt force vs. abdomen compression [Fixed-back belt loading tests: LC]

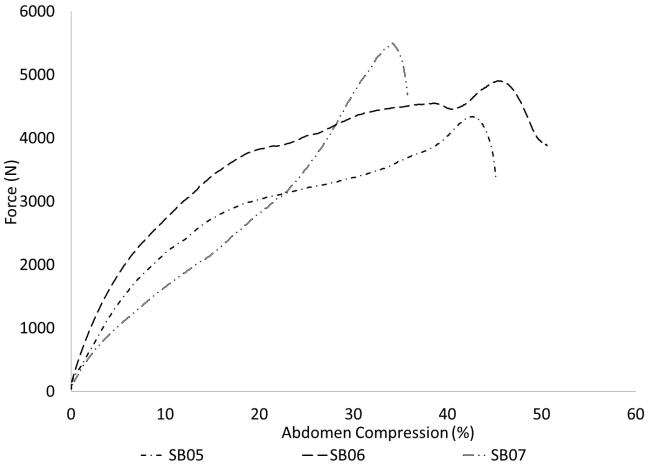

Fig. 4. Belt force vs. abdomen compression [Fixed-back belt loading tests: HC]

The injury findings during anatomical dissection performed following each fixed-back belt loading test to identify skeletal and abdominal injuries are tabulated in Table II. AIS3+ abdominal injuries were sustained in two of six specimens. In addition, five specimens sustained multiple rib fractures. While there were instances of skeletal injury, the analyses of biomechanical variables presented in this study apply only to abdominal soft tissue injuries.

TABLE II
INJURY SUMMARY (FIXED-BACK BELT LOADING)

Test #	Abdominal	AIS	Skeletal	AIS
SB01	None	0	None	0
SB02	None	0	Rib fractures: R 10; L 10	450202.2
SB03	None	0	Rib fractures: R 10; L 10, 11	450203.3
SB05	Ruptured kidney(R)	541640.4	Rib fractures: R 7, 8, 9, 10, 11;	450203.3
	Partial tear jejunum	541424.3	L 8, 9, 10, 11	
	Splenic capsule tear	544222.2		
SB06	Ruptured kidney(R)	541640.4	Rib fractures: R 6, 7, 8, 9, 10;	450203.3
	Full tear ileum	541426.4	L 6, 7, 8, 9, 10	
	Full tear duodenum	541024.4		
	Partial tear jejunum	541424.3		
SB07	None	0	Rib fractures: R 8, 9, 10, 11;	450203.3
			L 9, 10, 11	

Free-Back Rigid Bar Loading Test

Force vs. time and penetration vs. time histories for PMHS tests are presented in Figures B3 and B4. Peak impact forces ranged from 1.07 to 1.46 kN. The peak penetrations ranged from 72 to 122 mm. Peak compression of the abdomen ranged from 39 to 49%. The values of P_{max} in the IVC pressures ranged from 16.9 to 43.4 kPa. The $\dot{P}_{max}$ calculated for the IVC ranged from 1.11 to 5.47 kPa/ms, less than the 50% abdominal injury risk value of 9.3 kPa/ms suggested in [11].

Force vs. abdomen compression responses are shown in Figure 5 and impact force vs. abdomen penetration responses are shown in Figure B6. Again, the force and penetration data were not normalised since the specimens in the study closely matched the target demographic. In all tests, the ram displaced beyond the hard stop set at 27% of the abdomen depth. This was especially pronounced in test RB01. The reason for the excess penetration is attributed to the damping mechanism used to stop the impactor. A 55 mm thick medium density polyurethane foam was used in RB01 which was replaced with a 70 durometer Sorbothane rubber for tests RB02 and RB03. This overshoot occurred later in the event after the maximum force was recorded

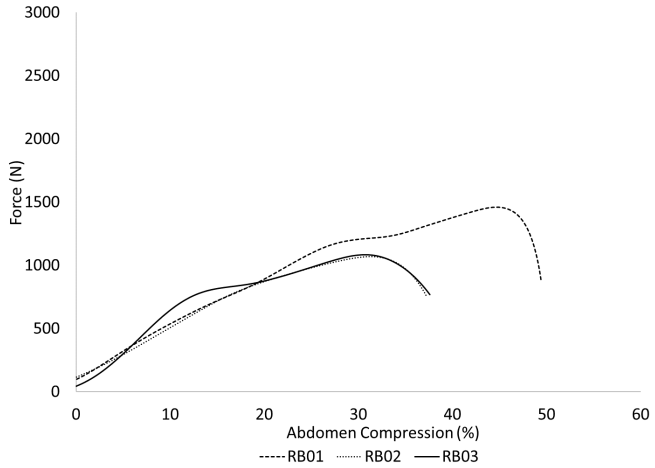

Fig. 5. Impact force vs. abdomen compression [Free-back rigid bar loading tests].

The anatomical dissection performed following each test revealed no injuries to any of the abdominal organs or other soft tissue. A fracture to the left fifth rib was identified in the RB01 specimen. The injury findings from the rigid bar loading tests are tabulated in Table III.

TABLE III
INJURY SUMMARY (ABBREVIATED INJURY SCALE 2005 - UPDATE 2008)

Test #	Abdominal	AIS	Skeletal	AIS
RB01	None	0	Rib fracture: L 5	450203.1
RB02	None	0	None	0
RB03	None	0	None	0

Biomechanical Variables

Table IV summerises the commonly accepted biomechanical variables for injury risk prediction calculated from all nine PMHS tests in the current study and corresponding peak values. Test SB07 resulted in an unusually high-pressure magnitude compared to other abdomen tests, likely due to the IVC being pinched between the thickly bound abdominal organ sack and the lumbar spine. Unfortunately, the test only included one pressure transducer in the IVC and could not be verified with a second measurement. However, the efficacy of the pressure transducer was verified for correctness after the completion of autopsy, and no transducer or measurement errors were identified, hence ruling out all measurement and data entry errors.

Biomechanical Targets

The biomechanical targets for small female-sized subjects under abdominal loading are presented as force-

compression corridors with mean and one standard deviation boundaries, as shown in Figures 6 and 7. The corresponding force-penetration and time-history response corridors are presented in Appendix C.

TABLE IV
SUMMARY OF PEAK RESPONSES AND CALCULATED BIOMECHANICAL PREDICTORS

Test	V_{max}	C_{max}	F_{max}	$(VC)_{max}$	$V_{max} * C_{max}$	$F_{max}*C_{max}$	P_{max}	$\dot{P}_{max}$	$P_{max}*\dot{P}_{max}$	Abdomen
	m/s	%	kN	m/s	m/s	kN	kPa	kPa/ms	kPa^2/ms	MAIS
Belt Loading (Lower-Compression)										
SB01	4.1	34	2.5	1.22	1.39	0.08	99.2	8.02	795.6	0
SB02	3.7	30	2.7	0.94	1.10	0.08	50.4	3.58	180.4	0
SB03	3.1	26	1.9	0.74	0.81	0.05	53.3	4.91	261.7	0
Average	***3.6***	***30***	***2.3***	***0.96***	***1.10***	***0.07***	***67.6***	***5.50***	***412.5***	
1 Std Dev	*0.5*	*4.0*	*0.4*	*0.24*	*0.29*	*0.01*	*27.3*	*2.27*	*334.1*	
Belt Loading (Higher-Compression)										
SB05	3.3	45	4.3	0.83	1.48	0.19	104.5	5.80	606.1	4
SB06	3.8	50	4.9	1.10	1.89	0.24	127.5	12.90	1644.8	4
SB07	3.1	36	5.5	1.04	1.12	0.20	245.0	31.50	7717.5	0
Average	**3.4**	**45**	**4.9**	**0.99**	**1.50**	**0.21**	**159.0**	**16.73**	**3322.8**	
1 Std Dev	0.3	7.1	0.6	0.14	0.38	0.02	75.3	13.27	3841.1	
Rigid Bar Loading										
RB01	5.9	49	1.5	1.73	2.99	0.71	43.4	2.52	109.4	0
RB02	5.9	38	1.1	1.56	2.25	0.41	24.7	2.88	71.1	0
RB03	6.1	40	1.1	1.66	2.35	0.43	17.6	5.47	96.3	0
Average	**6.0**	**42**	**1.2**	**1.65**	**2.53**	**0.52**	**28.6**	**3.63**	**92.3**	
1 Std Dev	0.1	5.8	0.2	0.08	0.40	0.16	13.3	1.60	19.4	

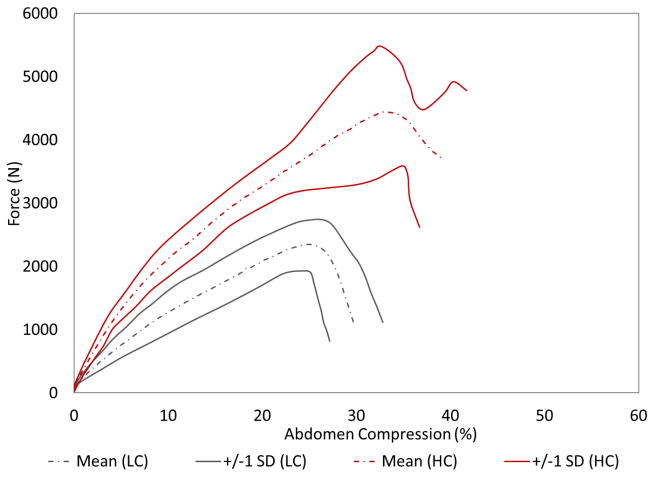

Fig. 6 Biomechanical targets: Fixed-back belt loading tests

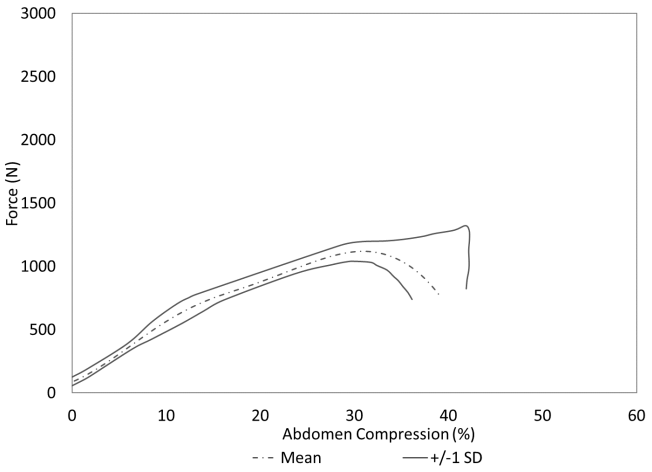

Fig. 7. Biomechanical target: Free-back rigid bar loading tests

IV. DISCUSSION

This study evaluated the abdominal responses of nine small female-sized PMHSs under belt pull and rigid bar impact loading conditions. Biomechanical targets were developed to benchmark the biofidelity of the abdomen in ATDs and HBMs.

Biomechanical Responses

This test series obtained biomechanical responses of small female PMHSs subjected to abdominal loading. For ATDs of comparable size to these test subjects, the resulting biomechanical responses can be compared directly (without scaling) when using the same test apparatus and methods. Additionally, the outcomes allow for direct

evaluation of small female human body models, without implementing scaling techniques.

The overall stiffness was greater in belt pull tests compared to rigid bar tests. This difference is likely because the back was constrained in the belt pull tests, and the belt distributed the load on the abdomen anterolaterally with less mobility of the specimen and the internal organs. In the rigid bar tests, the specimen was not constrained posteriorly. The impact area on the abdomen was smaller due to the shape of the impactor, allowing the abdomen to expand laterally.

One interesting finding in the belt pull tests was that the specimens in tests SB05 through 07, which were intended to produce injuries, showed stiffer responses compared to SB01-03. The differences in ram stroke may have been influenced by the combination of energy dissipated by the piston assembly pulling the seatbelt in addition to the mass recruitment and viscous properties of the PMHS abdomen. However, this should be further clarified by replacing the belt and specimen with a non-deformable mass in pull tests to exclude the abdomen characteristic as a variable. This type of analysis can isolate the effects of the piston assembly and stroke on the overall measurements.

When comparing within the cohort of SB05-07, test SB07 showed a softer initial response followed by a rapid increase in force. The abdominal organs had adhesions and were bound within thicker connective tissue, which may have led to decreased organ mobility or shifting within the thoraco-abdominal compartment resulting in a sudden mass recruitment effect upon engagement with anterior and lateral aspects of lumbar vertebrae. Two of the tests, SB06 and SB07, exhibited a rise-plateau-rise response possibly influenced by rib involvement.

The responses of the current small-statured subjects were compared to prior work on mid-sized males by scaling the force and penetration responses from [8] submarining tests and [3] mid-abdomen rigid bar impacts (Figures 8 and 9). Using abdominal depth as the characteristic dimension, the scaling factors for time, penetration and force applied were 0.78, 0.78 and 0.64, respectively [24]. The comparison of response data to the scaled Lamielle corridors is quite good for the lower compression tests (SB01-03). This is surprising in that the mean scaled penetration vs. penetration velocity from [8] suggests a rapid rise in penetration velocity compared to the current study (Figure B7), although the magnitudes are close. The scaling considers the abdomen impact condition as a spring-mass system, where a mass impacts the abdomen at a certain velocity. This assumption does not consider a gradual loading scenario such as a belt pull into the abdomen where the stiffness and damping characteristics of the abdomen play a prominent role. When comparing the rigid bar data with scaled Hardy corridors, the responses are generally characterised by rise to peak load followed by a drop with little change in penetration. However, the average stiffness observed in the current study was lower at 16.6 kN/m compared to approximately 20.5 kN/m in the Hardy study after scaling to small sized female.

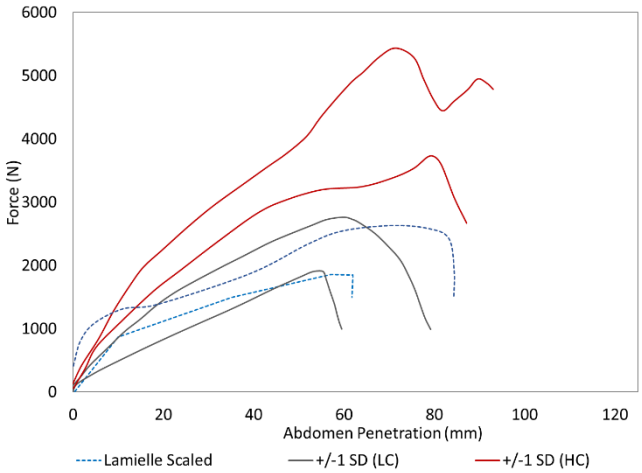

Fig. 8. Belt force vs. abdomen penetration targets compared to scaled Lamielle corridors.

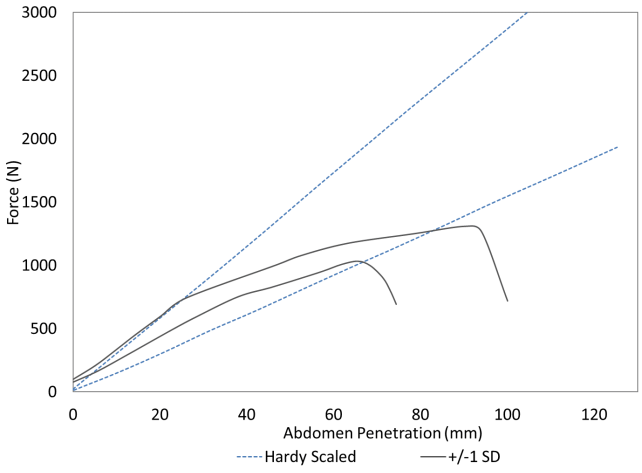

Fig. 9. Impact force vs. abdomen penetration targets compared to scaled Hardy corridors.

Injury Responses

Tests SB05 and SB06 resulted in right kidney ruptures, with damage through the renal cortex and medulla found superior to the renal pelvis, arteries, and veins. It is theorised that the ruptures were due to the kidneys being compressed as a result of loading from abdominal contents anteriorly, backplate posteriorly and the seatbelt laterally. Test SB05 also resulted in a splenic capsule tear that was found medially on the border of the renal and gastric surfaces. Both SB05 and SB06 resulted in jejunum injury of partial thickness on the non-

mesenteric side, which was identified in the path of belt loading. Additionally, SB06 resulted in ileum and duodenum injuries, although they were not directly in the path of belt loading. Since the bowels were not evacuated prior to testing the specimen in the current study, faeces were discovered at the injury location. By comparison, no kidney injuries were observed in the [8] submarining tests, although small intestine injuries and a subcapsular contusion of the spleen were identified, suggesting similarities in injury mechanisms. Similar injuries to the jejunum were found in [11] and [25] where the authors suggested that the presence of intestinal contents in the load path was potentially necessary to generate injury to the intestine. As the tissue and organs in the belt loading path displace, the bowel can get trapped between the belt and spine undergoing tension, generating a shear motion in the walls leading to tears in the jejunum. The peak compression in SB05 and SB06 were 45% and 50%, respectively, which fall in the range reported in previous studies required for creating tears to the jejunum-ileum.

SB07 did not result in abdominal organ injury, despite being in the test condition intended to be injurious. Fractures were observed in the lower level ribs, possibly due to belt engagement. The specimen in this test was 102 years old, the oldest specimen tested in the current or preceding abdominal trauma test series. The specimen's organs were adhered and bound within thicker connective tissue, which could not be identified during the specimen selection process using CT images. During impact, the authors speculate that this encapsulated sack deformed as a whole, thereby protecting the organs contained within. This likely contributed to increased stiffness of the abdomen resulting in a higher loading rate. Additionally, the combination of several lower rib fractures and the higher loading rate suggests that the liver, being the largest solid organ in this region, perhaps absorbed much of the belt forces without sustaining any injuries. Similar loading conditions have resulted in disparate liver injury outcomes in various studies using force, penetration, or combinations of those metrics. Reference [8] identified liver capsular tears at impact velocities of 4.6 and 4.9 m/s and forces of 3.7 and 4.8 kN respectively, however, no liver injuries were found in greater than 5.0 m/s tests with forces of 4.6 kN and above. Similarly, [25] found liver injuries in a test with seatbelt speed of 2.4 m/s and none in tests at 2.6, 2.7 and 2.8 m/s.

Biomechanical Variables

Table IV summerises the peak biomechanical responses recorded and calculated from the nine PMHS tests in the current study. The force and compression related responses and injury predictors were calculated based on non-normalised data since the specimens in the study closely matched the target demographic of a fifth percentile female. Reference [26] found that in seatbelt tests, a maximum compression of 48.4% was associated with the presence of AIS3+ lower abdominal injuries. In the current study, although peak compression of 45% and 50% resulted in AIS3+ injuries in belt pull tests, peak compression of 49% resulted in no abdominal injury in one of the rigid bar tests. This finding also highlights the variation in abdominal properties across the specimens and the small sample size in this study adds to this ambiguity.

In the same study [26], viscous criterion, $(VC)_{max,}$ of 1.4 m/s was associated with the presence of AIS4+ injuries. However, in the current study, $(VC)_{max}$ of 0.83 and 1.10 m/s resulted in AIS 3+ abdominal injuries while a $(VC)_{max}$ of 1.04 and 1.22 m/s resulted in no abdominal injury in the belt pull tests. Alternatively, the three rigid bar tests that resulted in no abdominal injury had $(VC)_{max}$ values between 1.56 and 1.73 m/s, suggesting that the metric is sensitive to loading mechanism. Viscous response varies based on loading rates, hence peak velocity and peak compression may occur at different times between impact and belt loading tests. In a rigid bar test, the peak velocity occurs at the time of impact and decreases thereafter as compression increases, whereas in the belt loading tests, the velocity increases with compression as the belt thrusts into the abdomen.

The abdominal injury criterion (AIC) proposed in [12-13] would account for this limitation by taking the product of maximum compression and velocity irrespective of their time of occurrence during an event. In the [11] study, $V_{max}*C_{max}$ values of 2.62 and 2.69 m/s resulted in AIS3+ abdominal injuries. These values were consistent with the 25% risk of AIS2+ injury proposed by [13], which corresponds to a $V_{max}*C_{max}$ of 2.52 m/s. However, in the current study, the $V_{max}*C_{max}$ values were 1.48 and 1.89 m/s for the two belt pull tests that resulted in AIS4+ abdominal injuries. Additionally, the rigid bar tests with no abdominal organ injury had AIC values between 2.25 and 2.99 m/s suggesting that the metric is not suitable for loading scenarios with high impact velocity but low compression.

The pressure-based metrics have shown potential in addressing these limitations while capturing injury information. Reference [11] suggested that IVC $\dot{P}_{max}$ of 9.3 kPa/ms corresponded to a 50% risk of AIS3+ abdominal organ injury. The findings in the current study agreed with the suggestion in all but one test (SB05) that resulted in AIS3+ abdominal injuries with a calculated IVC $\dot{P}_{max}$ value of 5.80 kPa/ms. The pressure readings may be

influenced by factors including vascular wall thickness in the region where the pressure transducer is placed, mobility of the organs to easily displace within the thoraco-abdominal cavity, and fluid flow into the numerous IVC tributaries. These factors are specimen-dependent and difficult to control. However, the threshold values may be adjusted as more data is collected and included in the development of new IRFs.

Some tests in the current study resulted in skeletal injuries but no abdominal injury. While factors contributing to skeletal injuries include bone mineral density (BMD) and subcutaneous tissue thickness, the same factors may not affect abdominal organ response. Tables II and III show discrepancies in skeletal and organ injuries corresponding to the same specimen. For instance, SB02 and SB03 resulted in AIS3+ skeletal injuries but no abdominal injury. Such a discrepancy is similar to previous findings [11][15], with pressure not being ideal for predicting injury to hard tissue, strengthening the basis to have separate skeletal thoracic and abdomen soft tissue injury metrics for ATDs.

$\dot{P}_{max}$ was found to be a strong predictor of AIS2+ and AIS3+ abdominal injury in past research [11][15] and supports suggestions made in other studies, such as the abdomen injury criterion ($AIC=V_{max}*C_{max}$, [12][13]), that abdominal injuries are rate dependent. The abdominal organs contain a membranous layer encompassing fluid within, like a water balloon, which may be ruptured when loaded with increasing force as the internal pressure exceeds the failure stress of the membrane. This suggests that the combination of the rate of pressure increase and the total pressure influences abdominal organ and soft tissue injuries.

Limitations

Selecting specimens that represent real-world occupants is challenging, especially when controlling for size and shape parameters. The current study accepted specimens in the normal BMI categories. It is worth noting that one of the specimens in the current test series included a male, primarily due to difficulty in procuring specimens within the anthropometric requirements.

The compression of the abdomen surpassed the intended target of 27% in both belt pull (SB01-03) and rigid bar (RB01-03) tests due to limitations in instrumentation and stopper mechanisms. In the belt pull tests, over-spooling out of the string potentiometer was observed due to inertial effects upon the sudden arrest of ram stroke resulting in higher displacement measurement. In the rigid bar tests, the stopper mechanism was ineffective in arresting the ram stroke upon reaching the target, however, such a sudden arrest would have damaged the system. While both these factors may be perceived as a confounding factor in response observed beyond the target, the data up to 27% abdominal compression in these tests are not influenced by these phenomena and considered valid.

Another challenge of working with abdominal responses and injury tolerances is the difficulty in categorising injury risk, largely due to the heterogeneity of the abdominal structure. The injury mechanisms may be different depending on the organ. While there is no obvious biomechanical relationship between the pressure reading in the abdominal vasculature and injuries observed, the pressure was found to be strongly correlated with organ injuries in both ex-vivo and in-vivo testing [11][14-15].

Another limitation of this study was the variation in the magnitude of pressure in test SB07. The test was operating with only one pressure transducer in the IVC with no redundant measures. It is unknown whether the high-pressure readings should be considered a true response or a reading generated by a contact-induced anomaly. This data point requires further investigation using statistical methods to assess its inclusion/exclusion in developing IRFs. Therefore, the pressure readings should be used with caution.

V. CONCLUSIONS

Three abdominal belt pull tests were conducted on three small PMHSs at a nominal velocity and abdominal compression of 4 m/s and 30%, respectively. Abdominal injury was not observed in any of the three tests. Peak seatbelt forces and penetrations ranged from 1.9 to 2.6 kN and 65 to 94 mm, respectively. Three abdominal belt pull tests were conducted on three small PMHSs at a nominal velocity and abdominal compression of 4 m/s and 45%, respectively. Abdominal injuries were identified in two of the three tests. Peak seatbelt forces and penetrations ranged from 4.4 to 5.5 kN and 70 to 118 mm, respectively. Three rigid bar loading tests were conducted on three small PMHSs at a nominal velocity and abdominal compression of 6 m/s and 42%, respectively. No abdominal injury was identified in these three tests. Peak impact forces ranged from 1.07 to 1.46 kN. The peak penetrations ranged from 74 to 122 mm. Finally, abdomen biofidelity response targets were created

for evaluating and improving the biofidelity of small female sized ATDs and HBMs.

VI. ACKNOWLEDGEMENT

This research was supported by the National Highway Traffic Safety Administration (NHTSA), USA, under Contract # DTNH2214D00348L; Task Order # DTNH2217F00157. Views contained within this manuscript are those of the authors and do not represent those of NHTSA. This study would not have been possible without the contributions of students, staff, and faculty in the Injury Biomechanics Research Center, USA, specifically Amanda Agnew, Akshara Sreedhar, Angela Tesny, Arri Willis, David Stark, Gretchen Baker, Julie Mansfield, Vikram Pradhan, and Zac Haverfield.

VII. REFERENCES

[1] Klinich KD, et al., Factors associated with abdominal injury in frontal, farside, and nearside crashes. Stapp Car Crash J. 2010
[2] Frampton R, Lenard J, Compigne S, An In-depth Study of Abdominal Injuries Sustained by Car Occupants in Frontal Crashes. Ann Adv Automot Med., 2012.
[3] Hardy WN, et al., Abdominal impact response to rigid-bar, seatbelt, and airbag loading. Stapp Car Crash J 45:1–41. 2001
[4] Trosseille X, et al., Abdominal response to high-speed seatbelt loading. Stapp Car Crash J 46:71–79, 2002
[5] Foster CD, et al., High-speed seatbelt pretensioner loading of the abdomen. Stapp Car Crash J 50:27–51, 2006
[6] Kent, Richard, et al., Biomechanical response of the pediatric abdomen, part 1: development of an experimental model and quantification of structural response to dynamic belt loading. Stapp car crash journal, 2006
[7] Uriot, J. et al., Investigations on the belt-to-pelvis interaction in case of submarining." Stapp car crash journal 50. 2006
[8] Lamielle S, et al., 3D deformation and dynamics of the human cadaver abdomen under seatbelt loading. Stapp Car Crash J. 2008
[9] Untaroiu CD, et al., Effect of seat belt pretensioners on human abdomen and thorax: biomechanical response and risk of injuries. J Trauma Acute Care Surg 72(5):1304–1315, 2012
[10] Le Ruyet A, et al., Effect of Abdominal Loading Location on Liver Motion: Experimental Assessment using Ultrafast Ultrasound Imaging and Simulation with a Human Body Model. Stapp Car Crash J. 2016
[11] Ramachandra et al., Biomechanical Responses of PMHS Subjected to Abdominal Seatbelt Loading, Stapp Car Crash J., 2016
[12] Rouhana, S.W., et al., Influence of velocity and forced compression on the severity of abdominal injury in blunt, nonpenetrating lateral impact. J. Trauma 25(6). 1985.
[13] Rouhana SW, et al., Biomechanical considerations for abdominal loading by seat belt pretensioners. Stapp Car Crash J. 2010
[14] Sparks JL, et al., Using pressure to predict liver injury risk from blunt impact. Stapp Car Crash J 2007
[15] Kremer MA, et al., Pressure-based abdominal injury criteria using isolated liver and full-body post-mortem human subject impact tests. Stapp Car Crash J. 2011
[16] Forman J, et al., Automobile injury trends in the contemporary fleet: Belted occupants in frontal collisions. Traffic Inj Prev. 2019
[17] Kahane, C. J., Injury vulnerability and effectiveness of occupant protection technologies for older occupants and women. (Report No. DOT HS 811 766). Washington, DC: National Highway Traffic Safety Administration. 2013
[18] Parenteau C, et al., Restrained Male and Female Occupants in Frontal Crashes: Are We Different?, IRCOBI. 2013
[19] Gayzik FS, et al., Development of the Global Human Body Models Consortium mid-sized male full body model. Injury Biomechanics Research Workshop. 2011
[20] Iwamoto M, et al., Development and Validation of the Total Human Model for Safety (THUMS) Toward Further Understanding of Occupant Injury Mechanisms in Precrash and During Crash. Traffic Inj Prev. 2015
[21] Mertz H, et al., The Hybrid III 10 Year Old Dummy, Stapp Car Crash Conference, 2001.
[22] Eppinger et al., Eppinger R, et al. "Development of Dummy and Injury Index for NHTSA's Thoracic Side Impact Protection Research Program," SAE 840885, 1984.

[23]Gennarelli TA, et al, The Abbreviated Injury Scale 2005 – Update 2008, Association for the Advancement of Automotive Medicine. 2008

[24]Lee, E. L., et al., Biomechanical response manual: THOR 5th percentile female NHTSA advanced frontal dummy, Revision 2 (Report No. DOT HS 812 811). Washington, DC: National Highway Traffic Safety Administration. 2020

[25]Howes MK, et al., Kinematics of the thoracoabdominal contents under various loading scenarios. Stapp Car Crash J. 2012

[26]Miller, M.A., The biomechanical response of the lower abdomen to belt restraint loading. Journal of Trauma 29(11). 1989

VIII. APPENDIX

Appendix A: Test Apparatus

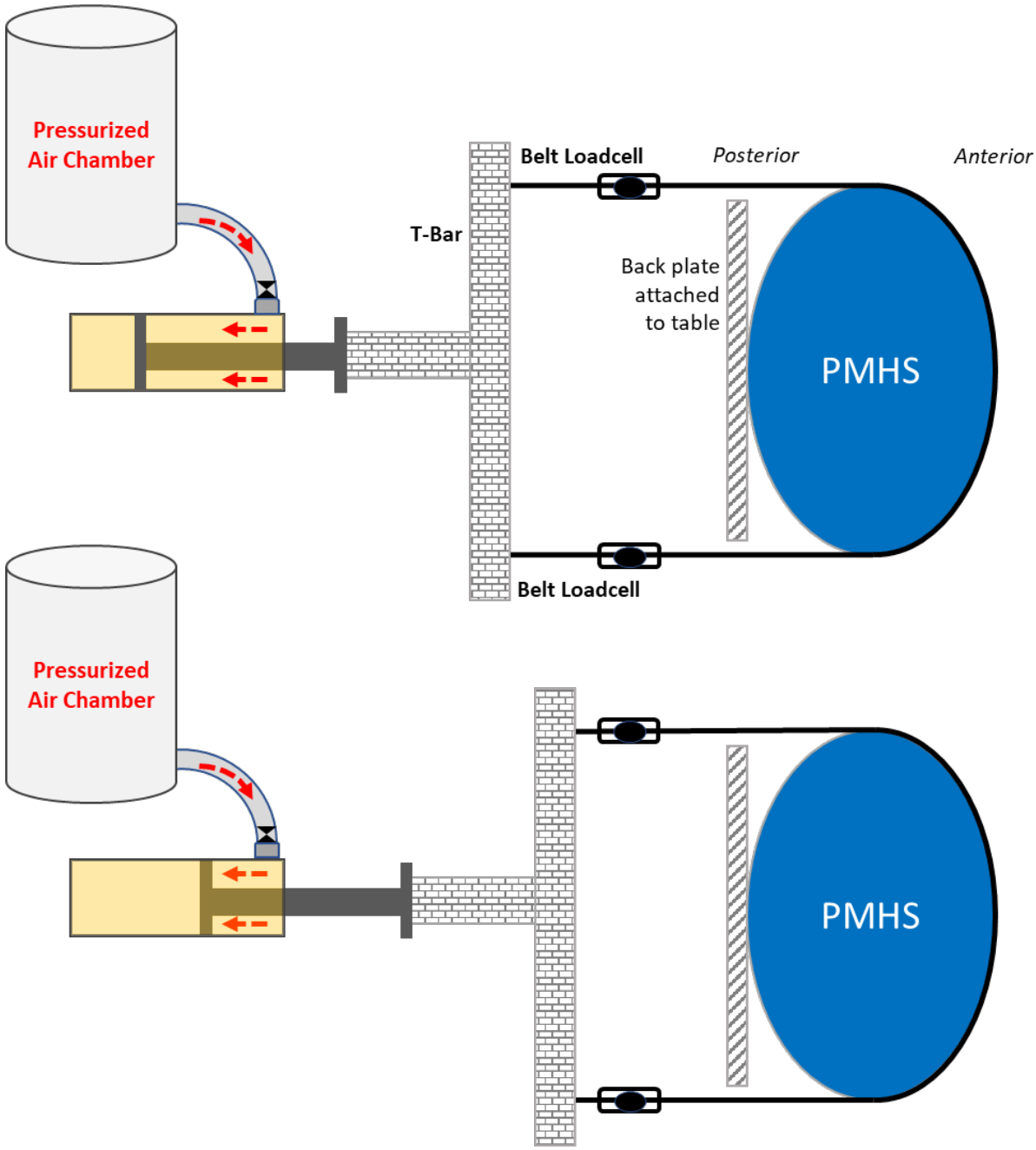

Fig. A1. Schematic of the fixed-back belt pull test setup; exemplary representation of starting positions of the ram (T-bar) for lower [top] and higher [bottom] compression tests. The test fixture utilised pressurised nitrogen to propel a piston, with a 4-inch bore and 10-inch stroke, rearward. This piston was connected to a T-bar mechanism, which also featured attachment points for a standard seatbelt. In order to vary the compression limit between the two series, the T-bar was pulled closer to the specimen and the belt length shortened. The placement of the PMHS and back constraint was not changed.

Appendix B: Biomechanical Responses

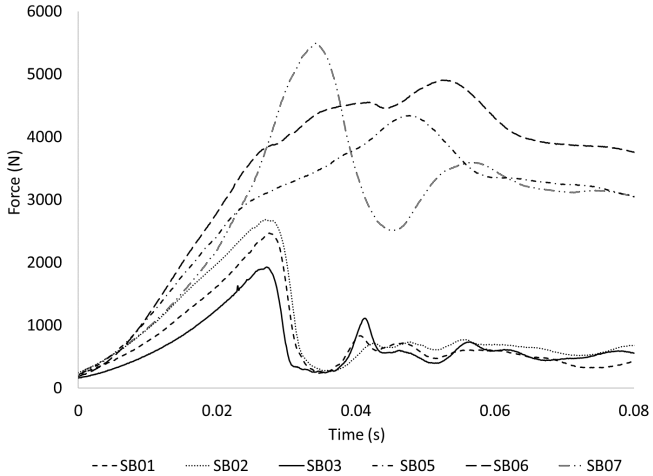

Fig. B1. Force-time histories from belt loading tests; [belt force, $F_{belt} = F_{left} + F_{right}$].

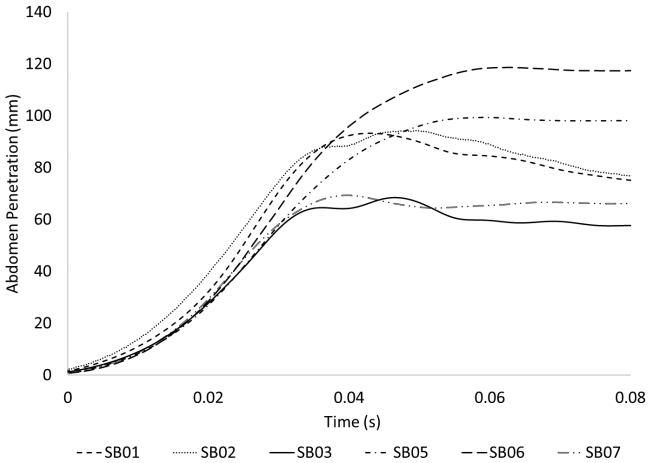

Fig. B2. Abdomen penetration-time histories from belt loading tests; [abdomen penetration, $\delta_{Abd} = \delta_{belt}$].

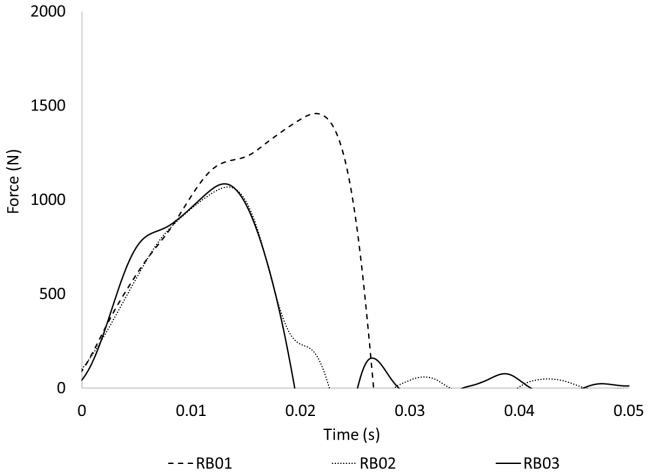

Fig. B3. Force-time histories from rigid bar loading tests; [ram force, $F_{Ram\ comp} = F_{Ram} - F_{Ram\ beyond\ loadcell}$].

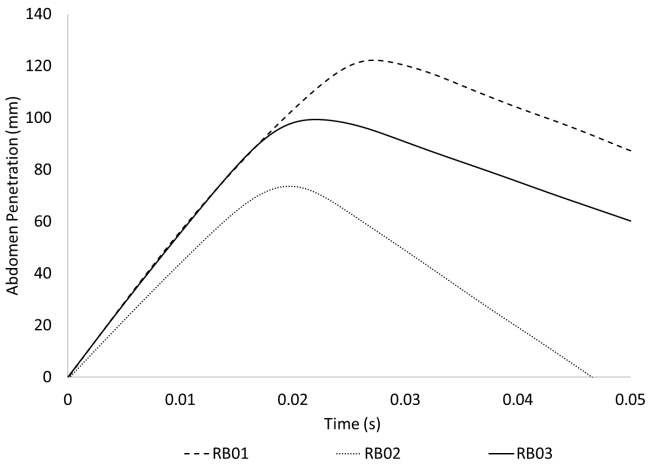

Fig. B4. Abdomen penetration-time histories from rigid bar loading tests; [abdomen penetration, $\delta_{Abd} = \delta_{Ram} - \delta_{L3}$].

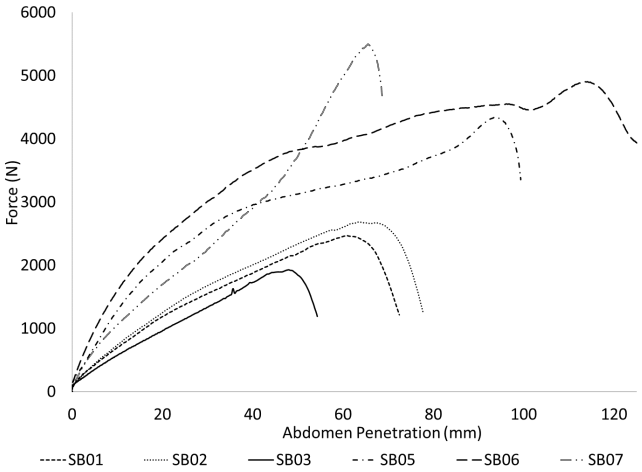

Fig. B5. Belt force vs. abdomen penetration from belt loading tests.

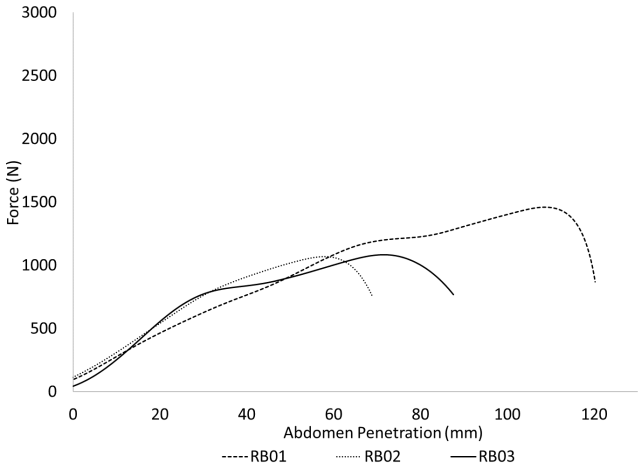

Fig. B6. Impact force vs. abdomen penetration from rigid bar loading tests.

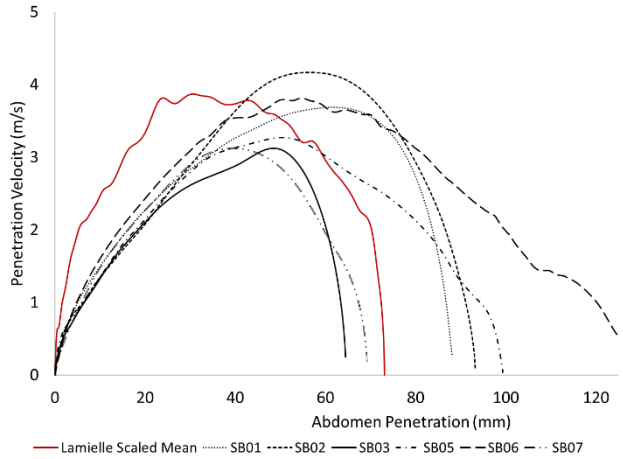

Fig. B7. Penetration vs. penetration velocity responses from belt loading compared to scaled Reference [8].

TABLE BI

PEAK PRESSURE RESPONSES AND CALCULATED RATE OF PRESSURE AT EACH SENSOR LOCATION

Test#	Sensor Location	P_{max} (kPa)	$\dot{P}_{max}$ (kPa/ms)	$P_{max} * \dot{P}_{max}$ (kPa^2/ms)
SB01	aorta_sup	40.5	2.61	105.7
	aorta_inf	sensor fail	-	-
	IVC_sup	17.5	0.84	14.7
	IVC_inf	99.2	8.02	795.6
SB02	aorta_sup	50.3	3.02	151.9
	aorta_inf	48.8	3.87	188.9
	IVC_sup	50.4	3.58	180.4
	IVC_inf	23.3	1.65	38.4
SB03	aorta_sup	36.0	3.52	126.0
	IVC_sup	46.9	3.05	143.0
	IVC_inf	53.3	4.91	261.7
SB05	aorta_sup	sensor fail	-	-
	aorta_inf	150.3	6.23	931.9
	IVC_sup	39.7	2.80	111.2
	IVC_inf*	104.5	5.80	606.1
SB06	aorta_sup	sensor fail	-	-
	aorta_inf	217.9	20.74	4510.5
	IVC_sup	60.8	4.73	285.8
	IVC_inf	127.5	12.90	1644.8
SB07	IVC_inf	245.0	31.50	7717.5
RB01	aorta_sup	24.5	1.52	37.2
	aorta_inf	39.6	9.22	365.1
	IVC_sup	21.5	1.11	23.9
	IVC_inf	43.4	2.52	109.4
RB02	aorta_sup	Sensor Fail	-	-
	aorta_inf	49.3	5.69	280.5
	IVC_sup	21.7	2.88	62.5
	IVC_inf	24.7	2.29	56.6
RB03	aorta_sup	12.6	0.57	7.2
	aorta_inf	21.1	1.77	37.3
	IVC_sup	17.6	5.47	96.3
	IVC_inf	16.9	1.95	33.0

Appendix C: Biomechanical Targets

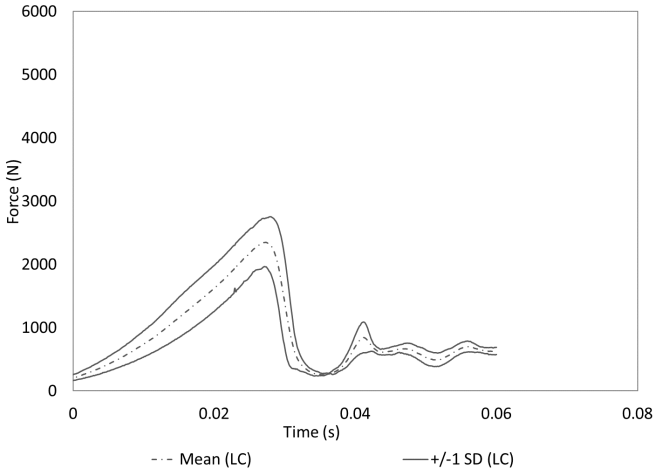

Fig. C1. Force-time targets from lower compression belt loading tests.

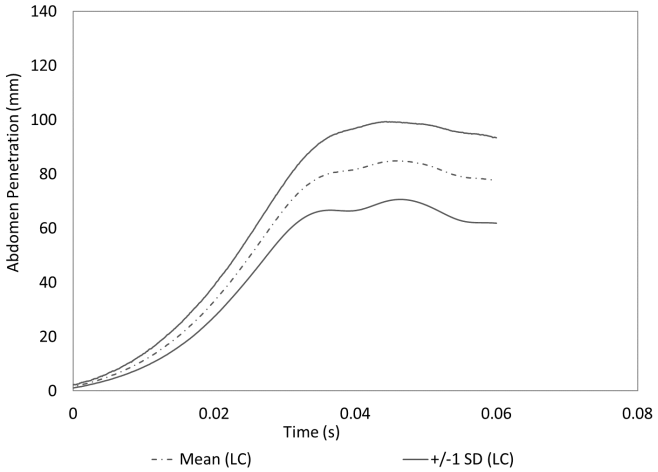

Fig. C2. Abdomen penetration-time targets from lower compression belt loading tests.

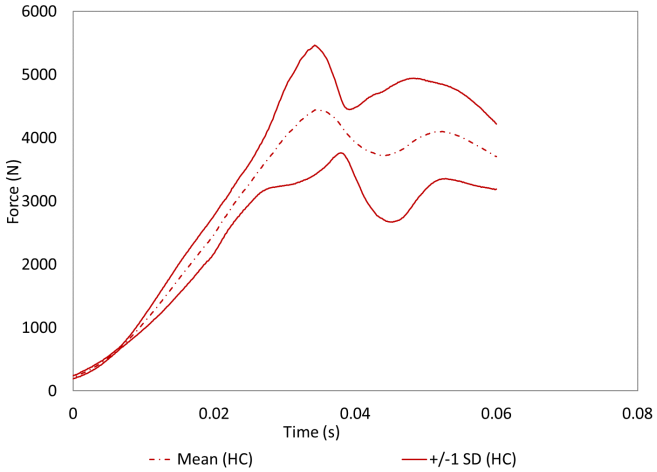

Fig C3: Force-time targets from higher compression belt loading tests

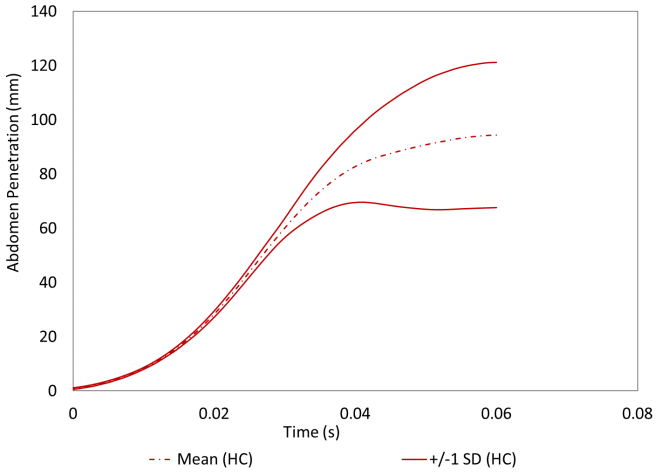

Fig C4: Abdomen penetration- time targets from higher compression belt loading tests

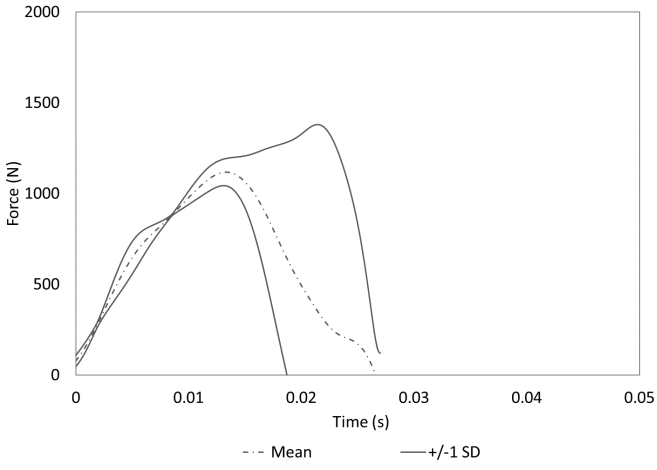

Fig. C5. Force-time targets from rigid bar loading tests.

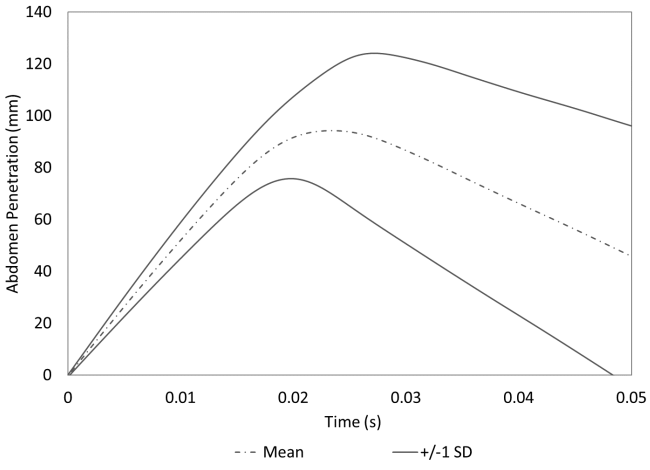

Fig. C6. Abdomen penetration-time targets from rigid bar loading tests.

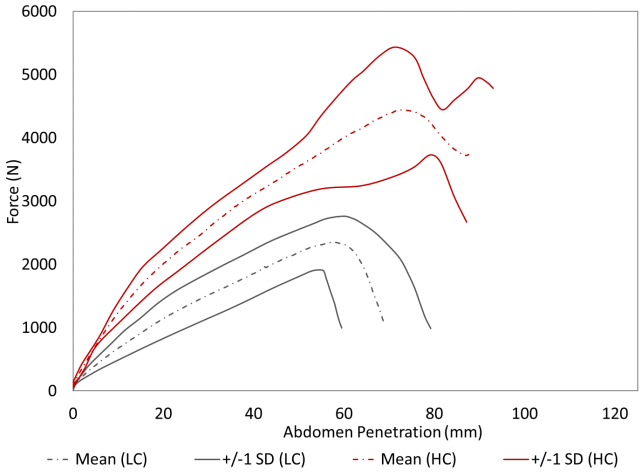

Fig. C7. Abdomen force-penetration targets from fixed-back belt loading tests.

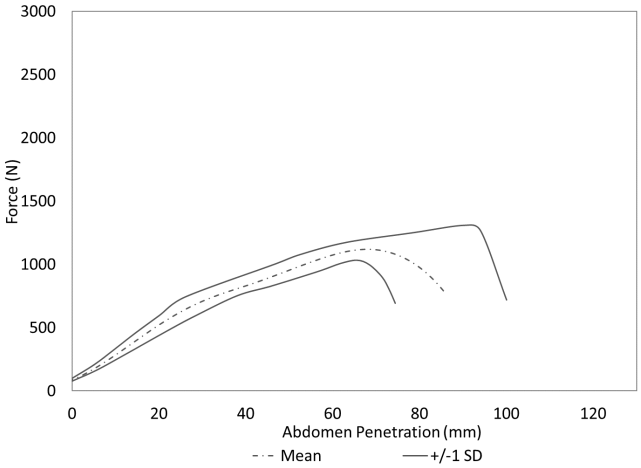

Fig. C8. Abdomen force-penetration targets from rigid bar loading tests.